DESY 95-020
TUM-T31-84/95
January 95

ISSN 0418-9833

Inclusive particle production in $p\bar{p}$ Collisions

F.M. Borzumati[1,2], G. Kramer[1]

[1] *II. Institut für Theoretische Physik*
Universität Hamburg, 22761 Hamburg, Germany

[2] *Institut für Theoretische Physik,*
Technische Universität München, 85747 Garching, Germany

Abstract

We calculate the inclusive production of charged hadrons in $p\bar{p}$ collisions to next-to-leading order (NLO) in the QCD improved parton model using a new set of NLO fragmentation functions for charged pions and kaons. We predict transverse-momentum distributions and compare them with experimental data from the CERN S$p\bar{p}$S Collider and the Fermilab Tevatron.

DESY 95-020
TUM-T31-84/95

1 Introduction

The inclusive production of single hadrons in hadron-hadron, photon-hadron and deep inelastic lepton-hadron collisions is an important area to test the QCD improved parton model. The inclusive cross section is expressed as a convolution of the parton distribution functions, the partonic cross sections and the fragmentation functions of quarks and gluons into charged or neutral particles. The factorization theorem ensures that parton distribution and fragmentation functions are universal functions and that only the hard scattering partonic cross sections change when different processes are considered. This theory provides a rather consistent description of many large-momentum-transfer-processes [1] and it is suitable for describing the inclusive production of single hadrons at large transverse momentum ($p_{\rm T}$) in various reactions. In this work we study the inclusive production of charged pions and kaons in high energy $p\bar{p}$ collisions.

Experimental data for charged single particle production come from the CERN ISR pp Collider [2]; from the UA1 [3] and UA2 [4] Collaborations at the S$p\bar{p}$S Collider at CERN; and from the CDF Collaboration at the Tevatron [5]. Recently, high statistics data from the UA1 MIMI Collaboration [6] have become available which has extended the $p_{\rm T}$ range to much larger values as compared to earlier UA1 analysis.

In [7], together with B.A. Kniehl, we already presented results for inclusive single-charged-hadron and single-π^0 cross sections at the next-to-leading order (NLO) [7]. We compared them with experimental data from the UA2 and CDF Collaborations. The overall agreement concerning the $p_{\rm T}$ dependence and the absolute normalization of the cross sections between theoretical and experimental results was satisfactory even for the smaller $p_{\rm T}$ region. An important drawback of this work, however, was due to the use of leading order (LO) parametrizations of fragmentation functions for charged pions and kaons [8]. These old parametrizations had been constructed more than ten years ago from fits to the data then available, obtained in low-energy e^+e^- annihilation experiments and deep inelastic muon-nucleon scattering.

Recently a NLO set of parametrizations for fragmentation into charged pions and kaons was obtained [9]. These parametrizations are generated through fits to e^+e^- annihilation data taken at $\sqrt{s} = 29\,\mathrm{GeV}$ by the TPC Collaboration. They produce rather satisfactory fits also for other e^+e^- data for charged particle production obtained at lower energy at DORIS and at higher energy at PETRA, PEP and LEP.

By using these new parametrizations, we are now in position to perform a full NLO calculation including NLO parton distribution functions, NLO parton-parton hard scattering cross sections and NLO fragmentation functions thereby, removing a serious limitation of our earlier work [7].

Other authors have almost simultaneously presented NLO parametrizations of fragmentation functions for light mesons, i.e. neutral pions [10], eta mesons [11] and charged pions [12]. In general these parametrizations are obtained through fits to data produced by the HERWIG Monte Carlo [13] at fixed $Q_0 = 30\,\mathrm{GeV}$. Parametrizations at lower scales are then obtained via NLO evolution. The authors of [10] and [11] compared their π^0–fragmentation functions with data from pp collisions in fixed target experiments and the ISR, and from $p\bar{p}$ collisions at the CERN S$p\bar{p}$S Collider. In [10] also, several sets of fragmentation functions for π^0 and η were obtained at a low scale, comparable to the one used in [8] through simultaneous fits to e^+e^- annihilation, fixed target and ISR pp collisions and S$p\bar{p}$S Collider data.

In this work we follow a different approach. We assume that the NLO fragmentation function for charged pions and kaons are sufficiently constrained by the fit to the TPC e^+e^- annihilation data and the fit to the gluon fragmentation function from the OPAL measurements [14]. Our aim is to verify whether the NLO parametrization of [9] gives also a satisfactory account of existing $p\bar{p}$ collider data and whether it improves the estimates obtained in our earlier work [7]. As in [7], we assume that the charged particle yield can be very well described by the sum of the pion and kaon yield and that the inclusive production of other charged particles, like p and $\bar{p}$ and heavier baryons is negligible compared to the production of the two lighter mesons.

This work is organized as follows. In Sect. 2 we give a short introduction of the formalism and fix our inputs. The results of our calculation and a comparison with data from $p\bar{p}$ colliders are presented in Sect. 3. This sections ends with a discussion of the results and concluding remarks.

2 Formalism and Input

Before presenting the results, we give a brief introduction to the NLO formalism. The NLO inclusive cross section for the production of a single hadron h in the reaction

$$p(p_1) + \bar{p}(p_2) \to h(p_3) + X\,, \tag{1}$$

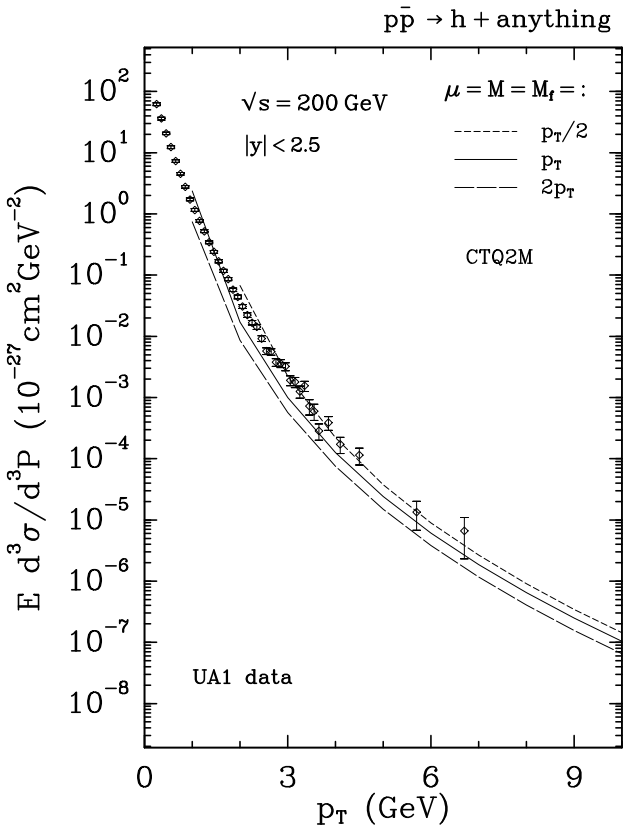

Fig. 1. Inclusive cross section for production of charged-hadrons ($h \equiv (h^+ + h^-)/2$) as a function of $p_{\rm T}$ for $\sqrt{s} = 200\,{\rm GeV}$ and rapidity $|y| < 2.5$. The short-dashed, solid and long-dashed lines correspond to the full NLO prediction for scales μ, M and M_f set equal to $p_{\rm T}/2$, $p_{\rm T}$ and $2p_{\rm T}$. For comparison, the UA1 data [3] taken at the same energy and in the same rapidity range are also shown

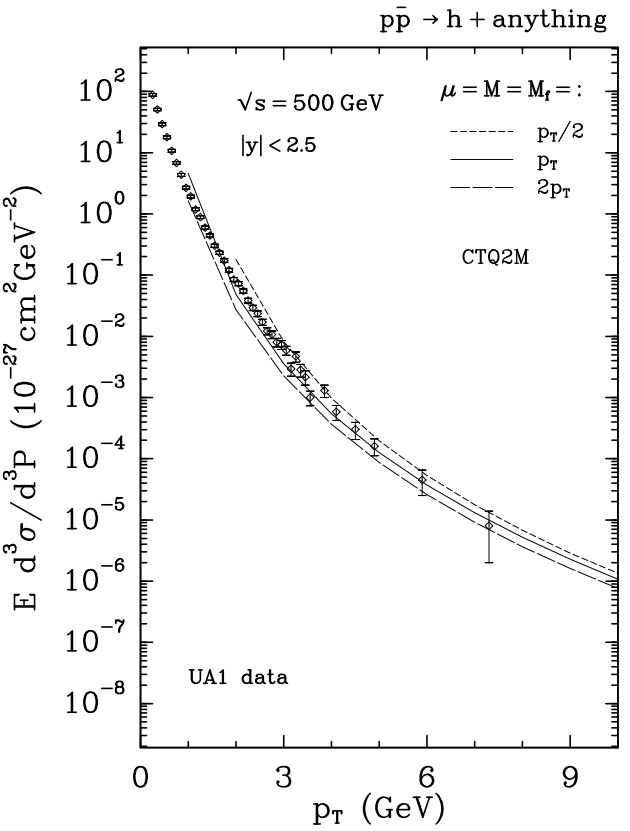

Fig. 2. Same as in Fig. 1 for $\sqrt{s} = 500\,{\rm GeV}$

is written as:

$$E_3 \frac{d^3\sigma}{d^3p_3} = \sum_{a,b,c} \int dx_1 \int dx_2 \int \frac{dx_3}{x_3^2}$$
$$\times F_a^p(x_1, M^2)\, F_b^{\bar{p}}(x_2, M^2)\, D_c^h\left(x_3, M_f^2\right)$$
$$\times \frac{1}{\pi S}\left[\frac{1}{v}\frac{d\sigma^0_{ab\to c}(s,v,\mu^2)}{dv}\,\delta(1-w)\right.$$
$$\left. + \frac{\alpha_{\rm s}(\mu^2)}{2\pi}\, K_{ab\to c}\left(s,v,w;\mu^2,M^2,M_f^2\right)\right]. \qquad (2)$$

The partonic variables v and w are related to the usual s, t, u ($s = (p_a + p_b)^2$, $t = (p_a - p_b)^2$ and $u = (p_b - p_c)^2$) as: $v = 1 + t/s$, $w = -u/(s+t)$. They are related to the hadronic variables $S = (p_1 + p_2)^2$, $T = (p_1 - p_3)^2$ and $U = (p_2 - p_3)^2$ by:

$$s = x_1 x_2 S\,, \qquad t = \frac{x_1}{x_3}\,T\,, \qquad u = \frac{x_2}{x_3}\,U\,, \qquad (3)$$

The indices a, b, c run over gluons and N_F flavours of quarks. As in our earlier work [7], we assume $N_F = 4$ and neglect the influence of the charm-quark threshold. $F_a^p(x_1, M^2)$ and $D_c^h(x_3, M_f^2)$ are the usual structure and fragmentation functions for partons of type a and c respectively inside the proton and the hadron h. They depend on x_1, x_3, the fractions of proton momentum carried by parton a and the fraction of the momentum of parton c carried by hadron h and on the factorization scales M and M_f. The additional mass parameter μ is the renormalization scale for the strong coupling. Finally, $d^3\sigma^0_{ab\to c}$ is the LO partonic cross section for the process $a + b \to c + X$ in $\mathcal{O}\left(\alpha_{\rm s}^2(\mu^2)\right)$. The $K_{ab\to c}$ functions are the NLO corrections to $a + b \to c + X$ and are taken from the work by Aversa et al. [15].

The form of the coefficients $K_{ab\to c}$ is not unique. They depend on the choice of finite corrections $f_{i,j}(x)$ and $d_{i,j}$ $(i, j = q, g)$ to structure and fragmentation functions. These subtraction terms are accompanied by appropriate definitions of the F_a^p and D_c^h. We choose here the structure functions in the $\overline{\rm MS}$ scheme. Specifically, we take the CTQ2M ($\overline{\rm MS}$) set of the proton distribution function from [16] which gives a good fit to recent structure function measurements at small x [17]. The starting scale of this set is $M_0 = 2\,{\rm GeV}$

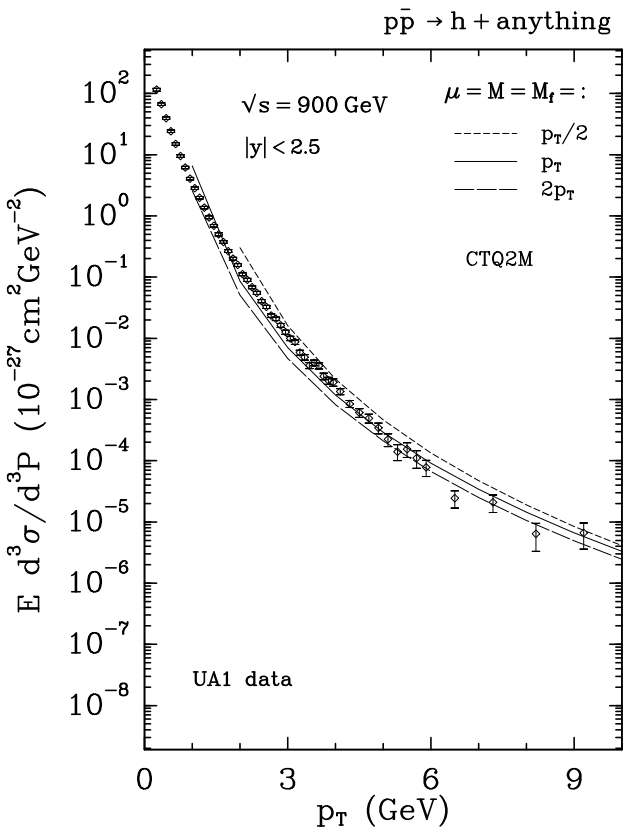

Fig. 3. Same as in Fig. 1 for $\sqrt{s} = 900\,\mathrm{GeV}$

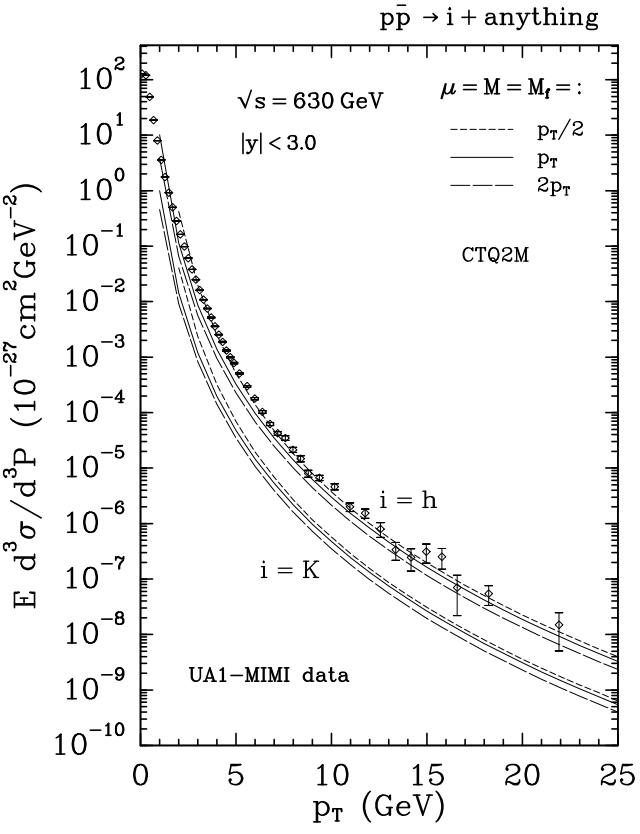

Fig. 4. Inclusive cross section for production of hadrons $h \equiv h^+ + h^-$ and kaons, $K \equiv K^+ + K^-$ as a function of p_{T} for $\sqrt{s} = 630\,\mathrm{GeV}$ and rapidity range $|y| < 3.0$. The data obtained by UA1 MIMI Collaboration [6] for production of hadrons are also shown

and therefore it can be used for prediction of the single particle cross section at fairly small values of p_{T}. The α_{s} is computed from the two-loop formula with $\Lambda_{\overline{\mathrm{MS}}} = 0.231\,\mathrm{GeV}$ as in the fit of the CTQ2M ($\overline{\mathrm{MS}}$) structure function.

As functions D_c^h, we employ the parametrizations by Binnewies et al. [9]. They are given separately for the average of charged pions and kaons, also in the $\overline{\mathrm{MS}}$ scheme. They are extracted from the e^+e^- data on inclusive production of pions and kaons at $Q = 29\,\mathrm{GeV}$ and found in agreement with the majority of the e^+e^- data in the energy range between 5 GeV and 91 GeV. The $\Lambda_{\overline{\mathrm{MS}}} = 0.19\,\mathrm{GeV}$ chosen for these fits is compatible with the $\Lambda_{\overline{MS}}$ in the proton structure function. The starting energy Q_0, where fragmentation functions have simple parametrizations, is chosen to be $Q_0 = \sqrt{2}\,\mathrm{GeV}$. The x and Q^2 dependence is then obtained by a NLO evolution.

The gluon fragmentation function into pions and kaons is poorely determined in these fits to e^+e^- annihilation data. This is due to the fact that the gluon participates in the process only at NLO. It has an appreciable impact on the cross section only at very small values of x, contributing mainly through the Q^2 evolution, due to its coupling to the singlet combination of quarks. Therefore the gluon parameters are correlated with the sea quark parameters and are not very well constrained by e^+e^- data. To fix them independently, the gluon fragmentation into charged particles is compared in [9] to the three-jet data of the OPAL Collaboration at LEP [16].

In an earlier attempt [17] when this last comparison was not made, an equally good description of all the other e^+e^- data used in [9] could be obtained with weaker gluon fragmentation functions. To show the gluon effect, we shall give for comparison, the inclusive charged particle cross section with the weaker gluon distribution of [7] for one of the $p\bar{p}$ energies.

Further details of the fragmentations and their parametrization as a function of Q^2 can be found in [9].

3 Numerical results

We are now in position to present our numerical results. We work in the $\overline{\mathrm{MS}}$ scheme with $N_f = 4$ active quark

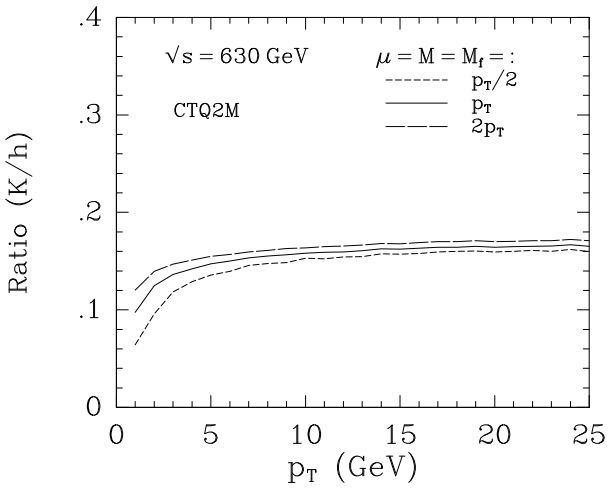

Fig. 5. The ratio of inclusive cross sections for charged K, $K \equiv K^+ + K^-$, over charged hadrons h, $h \equiv h^+ + h^-$, as a function of $p_{\rm T}$ for $\sqrt{s} = 630\,{\rm GeV}$ and $|y| < 3.0$

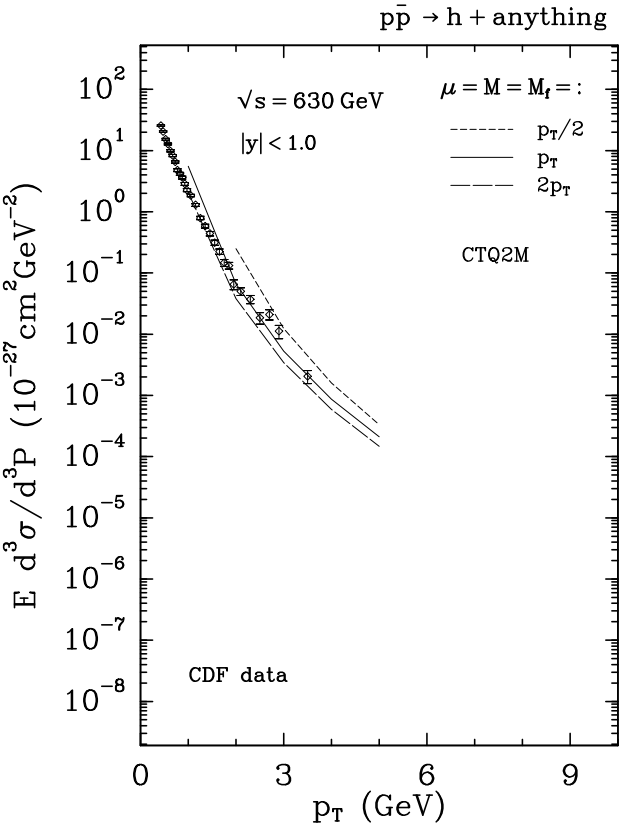

Fig. 6. Same as in Fig. 1 for $\sqrt{s} = 630\,{\rm GeV}$ and rapidity range $|y| < 1.0$. The theoretical results are compared with the data obtained by the CDF [5]

flavours. We set the three scales μ, M, M_f equal and we vary them between $p_{\rm T}/2$ and $2p_{\rm T}$. Unless otherwise specified the charged hadron h is defined as $h \equiv (h^+ + h^-)/2$, where $h^\pm$ sums over $\pi^\pm$ and $K^\pm$.

In Figs. 1,2 and 3 we show the inclusive charged hadron cross section for $p+\bar{p} \to h+X$ at $\sqrt{s} = 200, 500$ and 900 GeV. The rapidity is averaged over the interval $-2.5 < y < 2.5$. The agreement with the UA1 data [4] is best with scales equal to $p_{\rm T}$, except at $\sqrt{s} = 200\,{\rm GeV}$ where the data lie somewhat nearer to the prediction with scales equal to $p_{\rm T}/2$. In agreement with the experimental data, the theoretical curves show the expected increase of the high $p_{\rm T}$ tail between $\sqrt{s} = 200\,{\rm GeV}$ and $\sqrt{s} = 900\,{\rm GeV}$. According to [3], additional systematic errors due to luminosity and acceptance corrections are small ($\pm 15\%$). Therefore we can conclude that our predictions agree well in shape and normalization with the data. The data with small $p_{\rm T}$ have the smallest experimental errors. Unfortunately below $p_{\rm T} = 2$–$3\,{\rm GeV}$, our predictions cease to be valid: the soft production mechanism takes over while the hard production mechanism tends to give too fastly growing results.

The most recent and best experimental data come from the UA1 MIMI Collaboration [6]. They have the smallest experimental errors and extend earlier analysis of UA1 measurements to $p_{\rm T}$ values up to 25 GeV. These data are relative to production of charged hadrons h, with $h \equiv h^+ + h^-$. The theoretical predictions obtained for the same definition of h are plotted in Fig. 4 for scales $p_{\rm T}/2, p_{\rm T}$ and $2p_{\rm T}$, together with the data from [6]. The data and the theoretical predictions are for $\sqrt{s} = 630\,{\rm GeV}$ and are averaged over $|y| < 3.0$. The agreement with the data from the small up to the highest values of $p_{\rm T}$ is excellent. The curve with scale $p_{\rm T}/2$ fits the data best over the whole $p_{\rm T}$ range above $3\,{\rm GeV}$.

In Fig. 4 we give also our prediction for K production, in case such data become available in the future. The ratio to the total charge particle K/h is plotted in Fig. 5. Above $p_{\rm T} = 5\,{\rm GeV}$ this ratio is approximately constant in $p_{\rm T}$ with a slight increase towards larger $p_{\rm T}$. This ratio is approximately 0.15 and reflects the fact that the fragmentation of quarks and gluons into K mesons is much weaker than the fragmentation into pions. Since h is the sum of charged pions and kaons, the inclusive charged pion cross section can be computed easily from this ratio.

Similar conclusions can be drawn from the comparisons shown in Fig. 6 and 7 with CDF data [5] at $\sqrt{s} = 630\,{\rm GeV}$ and $\sqrt{s} = 1.8\,{\rm TeV}$, respectively. The definition of h is here again $h \equiv (h^+ + h^-)/2$. In both cases, the rapidity is averaged over the interval $-1 < y < 1$. The data at both energies agree and are predicted best with scales equal to $p_{\rm T}$.

Our calculation seems to provide a rather good description of data obtained in an energy range between

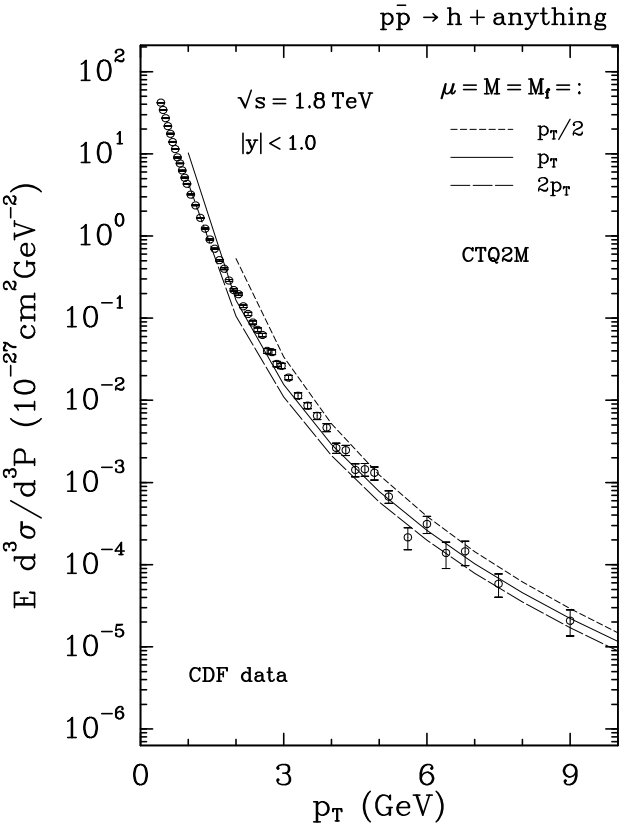

Fig. 7. Same as in Fig. 6 for $\sqrt{s} = 1.8\,\mathrm{TeV}$

200 GeV and 1.8 TeV, with an increase of energy by roughly one order of magnitude. Qualitatively our results are independent of $\sqrt{s}$ at small p_T, i.e. below 3 GeV, and increase with increasing energy in the large p_T-range, as it is characteristic for a hard-scattering cross section.

The degree of agreement between data and theoretical predictions, however, is rather difficult to assess by inspection of the logarithmic plots in Figs. 1-7, where the cross section drops rapidly over several orders of magnitude. It is clear that at small p_T, i.e. $p_\mathrm{T} < 3\,\mathrm{GeV}$, the theoretical curves deviate from the data. At higher p_T, unfortunately, the data points have larger errors and establishing the level of agreement becomes more problematic.

To make our comparison easier, we employ a three parameter fit to the data of the form

$$E\frac{d^3\sigma}{d^3p} = A\left(1 + \frac{p_\mathrm{T}}{p_{\mathrm{T}_0}}\right)^{-n}. \qquad (4)$$

In [3] the $\sqrt{s} = 500\,\mathrm{GeV}$ data of the UA1 Collaboration [3] have been fitted to (4). This fit yields the parameters $A = 408 \pm 24\mathrm{mb/GeV}^2$, $p_{\mathrm{T}_0} = 1.61 \pm 0.08\,\mathrm{GeV}$ and $n = 10.64 \pm 0.31$. We divide our theoretical predictions for the three choices of scales $p_\mathrm{T}/2$, p_T, and $2p_\mathrm{T}$ as well as the experimental data by the fit (4), taking for A, p_{T_0} and n the central values.

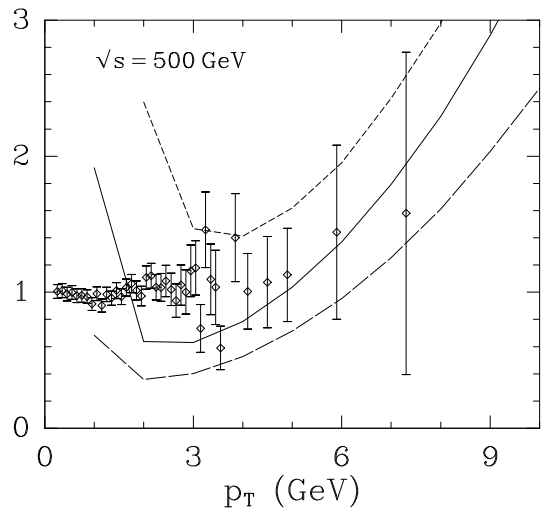

Fig. 8. The ratio theoretical cross section over fitted ansatz for the cross section as given by (4). The short-dashed, solid and long-dashed lines correspond to the NLO predictions from Fig. 2 for scales $\mu = M = M_f$ set equal to $p_\mathrm{T}/2$, p_T and $2p_\mathrm{T}$, compared to the ratio of experimental data points to fitted ansatz (4) from Fig. 2 ($\sqrt{s} = 500\,\mathrm{GeV}$, $|y| < 2.5$)

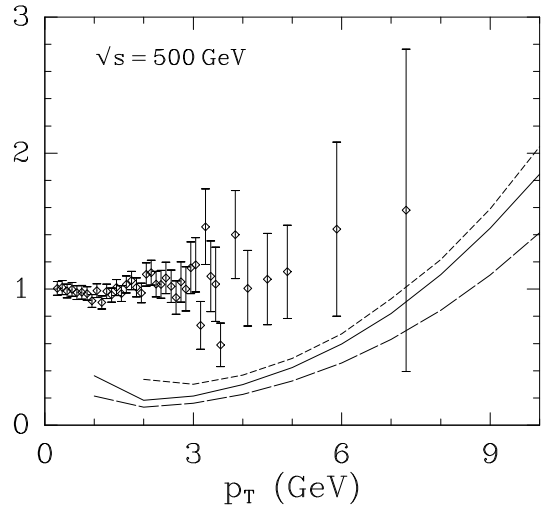

Fig. 9. Same as Fig. 8 for the weaker gluon fragmentation given in [17]

The result is shown in Fig. 8. It is clear that the fit reproduces the data rather well for $p_\mathrm{T} < 3\,\mathrm{GeV}$, but it is less satisfactory for p_T around 3–4 GeV. It is compatible with the data for the largest values of p_T only thanks to the very large error of these last data points. The ratio of the central value for the data over the fit (4) seems to show an increase for increasing p_T. This is the same behaviour shown by the theoretical

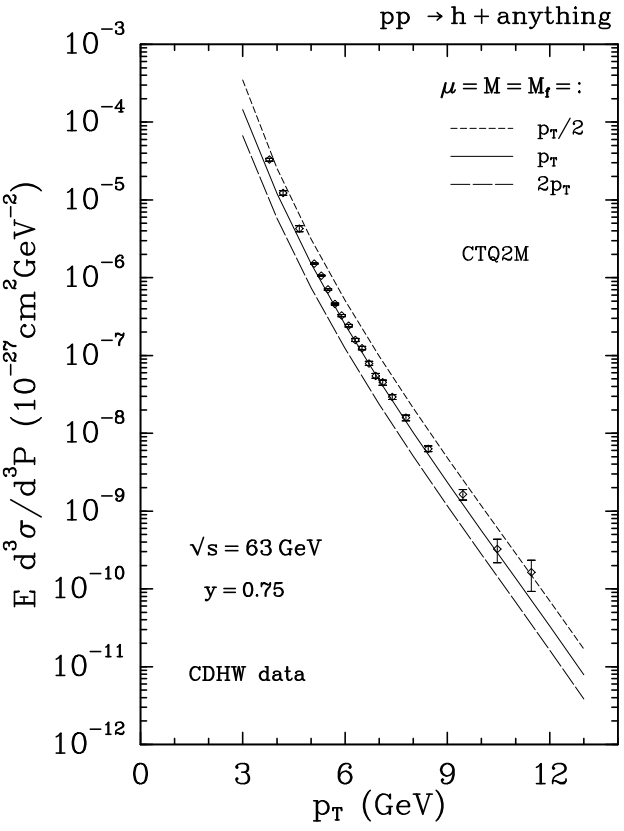

Fig. 10. Inclusive cross section for production of hadrons $h \equiv h^+ + h^-$ as a function of $p_{\rm T}$ for $\sqrt{s} = 63\,{\rm GeV}$ and rapidity $y = 0.75$. Also shown are the data obtained by the CDHW Collaboration [2] at the ISR pp collider

predictions for which the deviation from one becomes rather sharp at the largest values of $p_{\rm T}$ here considered. It is more visible from this figure what was previously said, i.e. that, overall, the choice of scales $\sim p_{\rm T}$ in our calculation seems to give the best agreement with the experimental data.

It would be interesting to see in this same type of plots the effect of different fragmentation functions. We do not attempt this here, but we show in Fig. 9 the same ratios obtained by using the parametrization of [17]. We remind here that this parametrization fits e^+e^- data (except for the gluon fragmentation function from the OPAL measurements [16]) equally well as the parametrization of [9]. The gluon fragmentation function in [17], however, is weaker than the one obtained in [9] where a fit to the OPAL data is also made. As one can see the results shown in Fig. 9 disagree with the data. The disagreement is stronger at smaller $p_{\rm T}$: the theoretical predictions are a factor 3–5 away from the data for $p_{\rm T} < 3\,{\rm GeV}$. A "strong" gluon fragmentation to charged pions and kaons is therefore needed to explain the inclusive charged particle cross sections in $p\bar{p}$ collisions.

So far all the inclusive particle production cross sections from $p\bar{p}$ are for the sum of all charged particles only. No separation into particle species has been done. Such cross sections exist at lower center of mass energies coming from the ISR pp collider [2]. These data are for charged pion production at $\sqrt{s} = 63\,{\rm GeV}$, $y \simeq 0.75$ and a range of $p_{\rm T}$ between 3 and 12 GeV. We have calculated this cross section with the same input as for the $p\bar{p}$ process (the $\bar{p}$ structure function in (2) is obviously replaced by the structure function for p). The result is shown in Fig. 10 together with the data from the CDHW Collaboration [2]. The agreement with the theoretical curve with scales equal to $p_{\rm T}$ is excellent over the whole range of $p_{\rm T}$.

We have calculated inclusive single-charged hadron cross sections in full NLO, by using NLO structure functions, NLO fragmentation functions for charged pions and kaons and NLO hard scattering cross sections. Our results were compared with experimental data from the CDHW, UA1, UA1-MIMI and CDF Collaborations. We found very good agreement, in particular with the UA1-MIMI data which have the smallest errors and extend over the largest $p_{\rm T}$ range. The agreement with the data is satisfactory for all center of mass energies between 63 GeV and 1800 GeV in shape and absolute normalization, even in the small $p_{\rm T}$ region. We have demonstrated that only those fragmentation functions with a large enough gluon contribution give a satisfactory account of the collider data. The strength of this gluon fragmentation function agrees with the OPAL data in the three-jet region sensitive to it [16].

Acknowledgments

The authors acknowledge the support from the Bundesministerium für Forschung und Technologie, Bonn, Germany, under contract 05 6 HH 93P(5), and of the EEC Program Human Capital and Mobility through Network Physics High Energy Colliders CHRX-CT93-0357 (DG 12 COMA). F.B. acknowledges also the support from the Bundesministerium für Forschung und Technologie, Bonn, Germany, under contract 06 TM 743.

References

1. J.F. Owens: Rev. Mod. Phys. 59 (1987) 465
2. D. Drijard et al., CDHW Coll.: Nucl. Phys. B208 (1982) 1
3. J.D. Dowell: in: 7th Topical Workshop on Proton-Antiproton Collider Physics, FNAL, 1988, R. Raja, A. Tollestrup, J. Yoh (eds.) Singapore: World Scientific 1988, p. 115; C. Albajar et al., UA1 Coll.: Nucl. Phys. B335 (1990) 261

4. M. Banner et al., UA2 Coll.: Phys. Lett. B122 (1983) 322 and Z. Phys. C27 (1985) 329
5. A. Para: in: 7th Topical Workshop on Proton-Antiproton Collider Physics, FNAL, 1988, R. Raja, A. Tollestrup, J. Yoh (eds.) Singapore: World Scientific 1988, p. 131; F. Abe et al., CDF Coll.: Phys. Rev. Lett. 61 (1988) 1819
6. G. Bocquet et al., UA1-MIMI Coll.: CERN preprint, CERN-PPE-94-47 (March 1994)
7. F.M. Borzumati, B.A. Kniehl, G. Kramer: Z. Phys. C57 (1993) 595
8. R. Baier, J. Engels, B. Petersson: Z. Phys. C2 (1979) 265; M. Anselmino, P. Kroll, E. Leader: Z. Phys. C18 (1983) 307
9. J. Binnewies, B.A. Kniehl, G. Kramer: DESY preprint, DESY 94-124 (July 1994)
10. P. Chiappetta, M. Greco, J.Ph. Guillet, S. Rolli, M. Werlen: Nucl. Phys. B412 (1994) 3
11. M. Greco, S. Rolli: Z. Phys. C60 (1993) 169
12. M. Greco, S. Rolli, A. Vicini: Z. Phys. C65 (1995) 277
13. G. Marchesini, B.R. Webber: Nucl. Phys. B238 (1984) 1, ibid. B310 (1988) 461
14. P.D. Acton et al., OPAL Coll.: Z. Phys. C58 (1993) 387
15. F. Aversa, P. Chiappetta, M. Greco, J.Ph. Guillet: Phys. Lett. B210 (1988) 225; ibid. B211 (1988) 465; Nucl. Phys. B327 (1989) 105
16. H.L. Lai, J.F. Botts, J. Huston, J.G. Morfin, J.F. Owens, J. Qiu, W.-K. Tung, H. Weerts: Michigan State University Report No. MSU-HEP-41024,CTEQ-404, October 1994.
17. I. Abt et al., H1 Coll.: Nucl. Phys. B407 (1993) 515; M. Derrick et al., Zeus Coll.: Phys. Lett. B 316 (1993) 412
18. J. Binnewies: Diploma thesis (May 1994)